Computational Analysis of Kilohertz Frequency Spinal Cord Stimulation for Chronic Pain Management

Scott F. Lempka, Ph.D., Cameron C. McIntyre, Ph.D., Kevin L. Kilgore, Ph.D., Andre G. Machado, M.D., Ph.D.

ABSTRACT

Background: Kilohertz frequency spinal cord stimulation (KHFSCS) is an emerging therapy for treating refractory neuropathic pain. Although KHFSCS has the potential to improve the lives of patients experiencing debilitating pain, its mechanisms of action are unknown and thus it is difficult to optimize its development. Therefore, the goal of this study was to use a computer model to investigate the direct effects of KHFSCS on specific neural elements of the spinal cord.

Methods: This computer model consisted of two main components: (1) finite element models of the electric field generated by KHFSCS and (2) multicompartment cable models of axons in the spinal cord. Model analysis permitted systematic investigation into a number of variables (*e.g.*, dorsal cerebrospinal fluid thickness, lead location, fiber collateralization, and fiber size) and their corresponding effects on excitation and conduction block thresholds during KHFSCS.

Results: The results of this study suggest that direct excitation of large-diameter dorsal column or dorsal root fibers require high stimulation amplitudes that are at the upper end or outside of the range used in clinical KHFSCS (*i.e.*, 0.5 to 5 mA). Conduction block was only possible within the clinical range for a thin dorsal cerebrospinal fluid layer.

Conclusions: These results suggest that clinical KHFSCS may not function through direct activation or conduction block of dorsal column or dorsal root fibers. Although these results should be validated with further studies, the authors propose that additional concepts and/or alternative hypotheses should be considered when examining the pain relief mechanisms of KHFSCS. **(Anesthesiology 2015; 122:1362-76)**

SPINAL cord stimulation (SCS) is the most common neurostimulation therapy to treat neuropathic pain conditions that are refractory to conventional medical management. Clinical SCS was first tested in 1967, and its demand has dramatically increased over the years with approximately 35,000 systems sold in 2008 alone.[1,2] SCS is a Food and Drug Administration–approved therapy, typically considered as a final treatment option, with a primary indication for refractory neuropathic limb pain. In the United States, SCS is primarily used to manage failed back surgery syndrome and complex regional pain syndrome.[3–5]

Although conventional SCS applied at a rate between 40 and 80 Hz has been a widely used clinical therapy for decades, it has a limited success rate (approximately 50% of patients receive ≥50% reduction in pain).[5] There has been recent interest in the use of much higher frequencies in an attempt to improve the clinical results with SCS. Kilohertz stimulation frequencies have shown the ability to generate rapid and reversible conduction block in peripheral nerve models[6–8] and have gained significant attention in recent years. Initial clinical data with a novel device capable of delivering kilohertz frequency SCS (KHFSCS) suggest promising clinical benefits and paresthesia-free effects.[9–12] These studies have also shown a patient preference for KHFSCS over conventional SCS and the ability of KHFSCS to provide pain relief

What We Already Know about This Topic

- Kilohertz frequency spinal cord stimulation (KHFSCS) may be an effective approach to controlling some forms of chronic pain
- Despite promising clinical results, the mechanisms of KHFSCS-mediated pain relief are unknown

What This Article Tells Us That Is New

- Using a computer model, it was shown that kilohertz frequency spinal cord stimulation (KHFSCS) used at clinical intensities probably does not cause the direct activation or conduction block of dorsal column or dorsal root fibers
- Possible sites of action for KHFSCS to be explored include synaptic terminals, cell bodies, and dendrites

Preliminary versions of the data in this article were presented in abstract and poster form at the following conferences: Mechanisms of Action: Electrical Stimulation of the Nervous System, March 28–30, 2014, Orlando, Florida; Society for Neuroscience Annual Meeting, November 15–19, 2014, Washington, D.C.; and North American Neuromodulation Society Annual Meeting, December 11–14, 2014, Las Vegas, Nevada.

Submitted for publication September 22, 2014. Accepted for publication February 24, 2015. From the Center for Neurological Restoration, Cleveland Clinic, Cleveland, Ohio (S.F.L., A.G.M.); Research Service, Louis Stokes Cleveland Veterans Affairs Medical Center, Cleveland, Ohio (S.F.L., C.C.M., K.L.K.); Department of Biomedical Engineering, Case Western Reserve University, Cleveland, Ohio (C.C.M., K.L.K.); Department of Orthopaedics, MetroHealth Medical Center, Cleveland, Ohio (K.L.K.); and Lerner Research Institute, Cleveland Clinic, Cleveland, Ohio (A.G.M.).

 Anesthesiology 2015; 122:1362-76

in patients who failed conventional SCS. However, results with KHFSCS remain inconsistent. A recent double-blind, placebo-controlled crossover trial concluded that KHFSCS was not better than sham treatment.[13]

The limited and contradictory clinical data available for KHFSCS emphasize the need for a detailed and systematic characterization of its therapeutic mechanisms that currently remain unclear. Several potential therapeutic mechanisms have been suggested: direct activation, conduction block, pseudospontaneous activation, transmission delays, or conduction failure at branch points.[8,14,15] Direct conduction block of action potentials is often considered the most logical mechanism because therapeutic KHFSCS does not produce paresthesias.[9–12]

To determine the pain relief mechanisms of KHFSCS, we must understand the electric fields generated by the stimulation waveform and its direct effects on the neural elements of the spinal cord. This knowledge can be difficult to gain experimentally, and, in the past, several groups have used computational models to study conventional SCS.[16–23] The goal of this study was to use similar theoretical techniques to investigate the effects of KHFSCS on the spinal cord. Our model infrastructure consisted of a finite element model (FEM) of an SCS lead implanted in the epidural space along with multicompartment cable models of dorsal root (DR) and dorsal column (DC) fibers in the spinal cord. This approach permitted systematic characterization of numerous variables and their influence on the direct effects of KHFSCS: waveform shape, dorsal cerebrospinal fluid (dCSF) thickness, lead location, fiber collateralization, and fiber size. The data indicate that direct activation of the spinal cord elements may be possible with KHFSCS; however, it is unlikely that clinical KHFSCS generates direct conduction block within the spinal cord.

Materials and Methods

We used computer models to investigate the direct response of spinal cord axons to KHFSCS used in chronic pain management. The computer models had two main components: (1) FEM of an SCS lead implanted in the epidural space and (2) electrical models of spinal cord axons. We performed the model analysis in three steps: (1) from the FEM, we calculated the extracellular voltages generated in the spinal cord and surrounding tissue during KHFSCS; (2) we generated electrical models of axons within the spinal cord; and (3) we assessed the direct axonal response to KHFSCS by applying the extracellular voltages (step 1) to the axon models (step 2). The text below provides an overview of these modeling procedures (see the appendix for a detailed description of the modeling parameters).

Step 1: Calculate the Extracellular Voltages Generated by KHFSCS

The first step in our model analysis was to estimate the extracellular voltages generated in the spinal cord during KHFSCS. We performed this estimation using finite element analysis. Finite element analysis is a computerized method for predicting how an object (*i.e.*, the spinal cord and surrounding tissue) reacts to various forces (*i.e.*, the electric fields generated during KHFSCS).[24] In finite element analysis, the object is represented by thousands-to-millions of geometrical shapes or finite elements, such as tetrahedrons. Mathematical equations containing information (*i.e.*, electrical conductivity) connecting each point in the object are then used to estimate the response (*i.e.*, extracellular voltage) of each finite element. A computer then sums the response of each individual element to estimate the response of the complete object.

To perform this analysis, we created a three-dimensional FEM of the lower thoracic spinal cord and its surrounding anatomy (fig. 1A). The FEM consisted of the gray and white matter of the spinal cord, surrounding cerebrospinal fluid, dura, epidural fat, vertebral bone, and a surrounding general thorax layer. The dimensions of the spinal cord and the white and gray matter boundaries were defined by human cadaver samples of the lower thoracic spinal cord.[25] The FEM also contained an explicit representation of an eight-electrode percutaneous lead implanted in the epidural fat dorsal to the spinal cord. The electrode was placed on the dorsal surface of the dura along the spinal cord midline. Electrical conductivities were assigned to each domain based on experimental data available in the literature (Table 1).[21,22,26] In this study, all simulations were performed for bipolar stimulation with a separation of 8 mm center-to-center between active electrodes (fig. 1A).

The extracellular voltages generated during KHFSCS were the output of this first step in the model analysis. To calculate the voltage at each point in the model tissue, we placed current sources at the appropriate stimulating electrodes, set the outer model surface to ground (*i.e.*, 0 V) and then solved the Poisson equation. These tissue voltages were then interpolated onto the spinal cord axon models described below (step 2).

Step 2: Define Axon Models in the Spinal Cord

The second step of our model analysis was to define computer models of spinal cord axons. The fundamental purpose of SCS is to modulate neural activity with electric fields. Theoretical and experimental studies have demonstrated that axonal activation is the principal effect of stimulation within the central nervous system.[27] With regard to SCS, studies have shown that the two axon types most likely affected by SCS are the large-diameter myelinated DR fibers and Aβ fibers within the DCs.[21,28] Therefore, we included computer models of both DR and DC fibers in our analysis (fig. 1B). DC and DR fibers were represented by a previously published compartmental model of a mammalian axon.[29] In this axon model, the nodes of Ranvier contained active (*i.e.*, voltage-gated fast Na^+, persistent Na^+, and slow K^+ ion channel conductances) and passive (*i.e.*, leak conductance, capacitance) membrane properties.

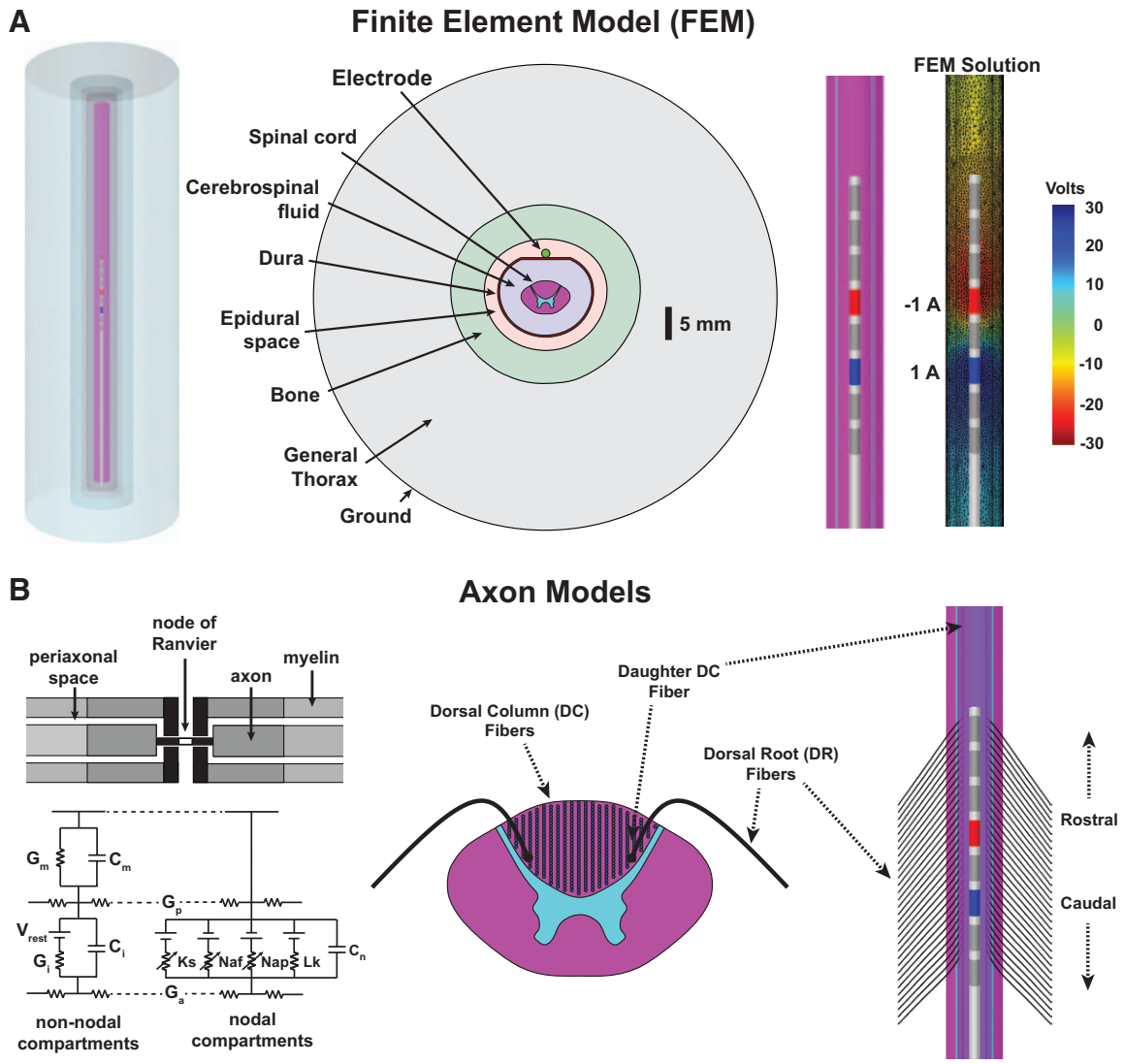

Fig. 1. Computer model of kilohertz frequency spinal cord stimulation (KHFSCS). (*A*) A finite element model (FEM) was created of the lower thoracic spinal cord and surrounding anatomy along with a KHFSCS lead implanted in the epidural space. The figure in the *upper right corner* shows the voltage distribution generated by bipolar stimulation with a +1 A current applied at the contact shown in *blue* (anode) and –1 A current applied at the contact shown in *red* (cathode). (*B*) Multicompartment cable models of the dorsal column (DC) and dorsal root (DR) fibers were included in this analysis and were based on a previously published model of a mammalian myelinated axon.[29] DR fibers consisted of a mother fiber and a bifurcated daughter fiber running along the DC.[22] The three-dimensional trajectory of the DR mother fiber approximated the anatomy of dorsal rootlets in the lower thoracic spinal cord.[20,30]

DC Fibers. Dorsal column fibers, running longitudinally along the rostrocaudal axis, were placed on a regular grid (200 μm for the mediolateral direction and 100 μm for the dorsoventral direction) within the white matter boundary of the DC defined by the FEM.[22]

DR Fibers. Dorsal root fibers had a three-dimensional axon trajectory in which they entered the spinal cord at a 45-degree angle with respect to the transverse plane and approximated the anatomy of the dorsal rootlets in the lower thoracic spinal cord.[20,30] DR fibers were placed in 1-mm intervals along the rostrocaudal axis (fig. 1B). Near the dorsal horn of the spinal cord, the DR fiber branched into a daughter fiber that traveled along the rostrocaudal axis within the DC.[22]

Step 3: Assess the Direct Axonal Response to KHFSCS

The third step in our model analysis was to assess the direct axonal response to KHFSCS. We performed this final step by applying the extracellular voltages (step 1) to the axon models of DC and DR fibers (step 2). We then calculated the stimulation amplitudes required for activation and conduction block under a variety of model parameters.

Outcome Measures. We calculated the minimum stimulation amplitudes required to generate action potentials (*i.e.*, activation threshold) and to block the conduction or propagation of action potentials along the axon (*i.e.*, block threshold) for an individual fiber. We defined thresholds as the peak amplitude for a single phase of the symmetric biphasic KHFSCS waveforms (fig. 2C).

Table 1. Electrical Conductivities Used in the Finite Element Model

Tissue	Conductivity (S/m)
White matter (longitudinal)	0.600
White matter (transverse)	0.083
Gray matter	0.230
Cerebrospinal fluid	1.700
Dura	0.600
Epidural fat	0.040
Vertebral bone	0.020
General thorax	0.250
Electrode contact	5.000E+06
Electrode insulation	1.000E-06

Activation Threshold. The activation threshold was defined as the minimum peak amplitude required to generate one or more action potentials in a particular fiber (fig. 2C).

Block Threshold. It is important to note that, unlike conventional (approximately 50 Hz) SCS, KHFSCS has the potential to block action potential conduction along an axon.[8] The block threshold was defined as the minimum peak amplitude required to block the conduction of an action potential from one end of an axon to the opposite end. To calculate the block threshold, an internal stimulating electrode was placed at one end of an axon (*i.e.*, most caudal node of a DC fiber) and was used to apply a test pulse after a KHFSCS waveform had been applied for 40 ms. Successful conduction block was defined as the condition in which no action potential propagated from the caudal end of the axon to the rostral end (fig. 2C).

Model Investigations. We varied a number of model parameters to investigate their potential significance in KHFSCS. These parameters included waveform shape, dCSF layer thickness, lead location, fiber collateralization, and fiber size (Table 2). To examine the potential influence of each parameter, we calculated the activation and conduction block thresholds for DC and DR fibers for each parameter set.

Waveform Shape. We considered two KHFSCS waveforms in this study. The first KHFSCS waveform was a continuous 10-kHz sinusoidal waveform. The second KHFSCS waveform was a rectangular waveform with symmetric cathodic and anodic phases with a pulse width of 30 μs and an interpulse interval of 20 μs applied at a rate of 10 kHz. This rectangular KHFSCS waveform closely resembled the reported waveform parameters of the Senza device manufactured by Nevro, Inc., USA.[10] We also calculated activation thresholds for a conventional SCS waveform with a pulse width of 210 μs applied at a rate of 50 Hz, which represented common clinical stimulation parameters.[31–33]

dCSF Layer Thickness. In this study, the dCSF layer thickness represented the distance between the dorsal surface of the spinal cord and the dural sac. KHFSCS thresholds were calculated for dCSF thicknesses of 2.0, 3.2, and 4.4 mm.

Lead Location. We defined lead location as the position of the lead relative to the dural surface and the spinal cord midline. To examine the effects of dorsoventral lead position on KHFSCS thresholds, we initially placed the lead on the dural surface at the spinal cord midline and moved it in the dorsal direction, that is, away from the dura. We calculated thresholds for distances of 0.0, 0.2, 0.4, 0.8, and 1.2 mm between the dura and the lead. To examine the effects of mediolateral lead position on KHFSCS thresholds, we again placed the lead at the spinal cord midline and moved it laterally along the surface of the dura. We calculated thresholds for lead positions offset 0.0, 1.0, 2.0, and 3.0 mm relative to the spinal cord midline.

Fiber Collateralization. We added collaterals to DC fibers to assess the effects of fiber collateralization or branching on KHFSCS thresholds. The branched DC fibers consisted of a parent fiber projecting along the rostrocaudal axis and daughter branches connected near the center of the parent fiber. The daughter collaterals were oriented perpendicular to the parent DC fiber and projected in the ventral direction. We calculated KHFSCS activation thresholds for DC fibers with a single collateral as well as DC fibers with multiple collaterals placed at adjacent nodes of Ranvier. We also examined multiple parent fiber-to-collateral diameter ratios (1.0, 1.6, and 2.0), multiple fiber diameters (5.7 to 16.0 μm), and KHFSCS with a monopolar stimulation configuration. The membrane surface area of branching nodes was increased to 150% relative to nonbranching nodes.[19] The DC parent fibers had a length of approximately 120 mm with node spacing dependent on the axon diameter.[29] The collateral length and node spacing were also diameter dependent with lengths of 4.5, 4.5, and 3.8 mm for collateral diameters of 5.7, 7.3, and 11.5 μm, respectively.

Fiber Size. We also varied the diameter of DC fibers to investigate the effects of fiber size on KHFSCS thresholds. We calculated activation and conduction block thresholds for three fiber diameters: 7.3, 11.5, and 15.0 μm.

Results

Waveform Shape

Several clinical and experimental studies have investigated the effects of kilohertz frequency electrical stimulation on the nervous system with stimulation waveforms having different parameters (*e.g.*, sinusoidal *vs.* rectangular; monophasic *vs.* biphasic; continuous *vs.* discontinuous; voltage controlled *vs.* current controlled).[6–8,10,13–15,34] We elected to focus our analysis on the waveforms that we believed were most relevant to current clinical applications of kilohertz frequency stimulation for chronic pain applications. Therefore, we considered continuous current-controlled sinusoidal and rectangular KHFSCS waveforms to examine the potential effects of waveform shape on activation and block thresholds (fig. 3). Both KHFSCS waveforms were applied at a rate of 10 kHz. We also considered a conventional SCS waveform applied at a rate of 50 Hz.

The activation and conduction block thresholds for both KHFSCS waveforms and the activation thresholds for the conventional SCS waveform were calculated for all DC and

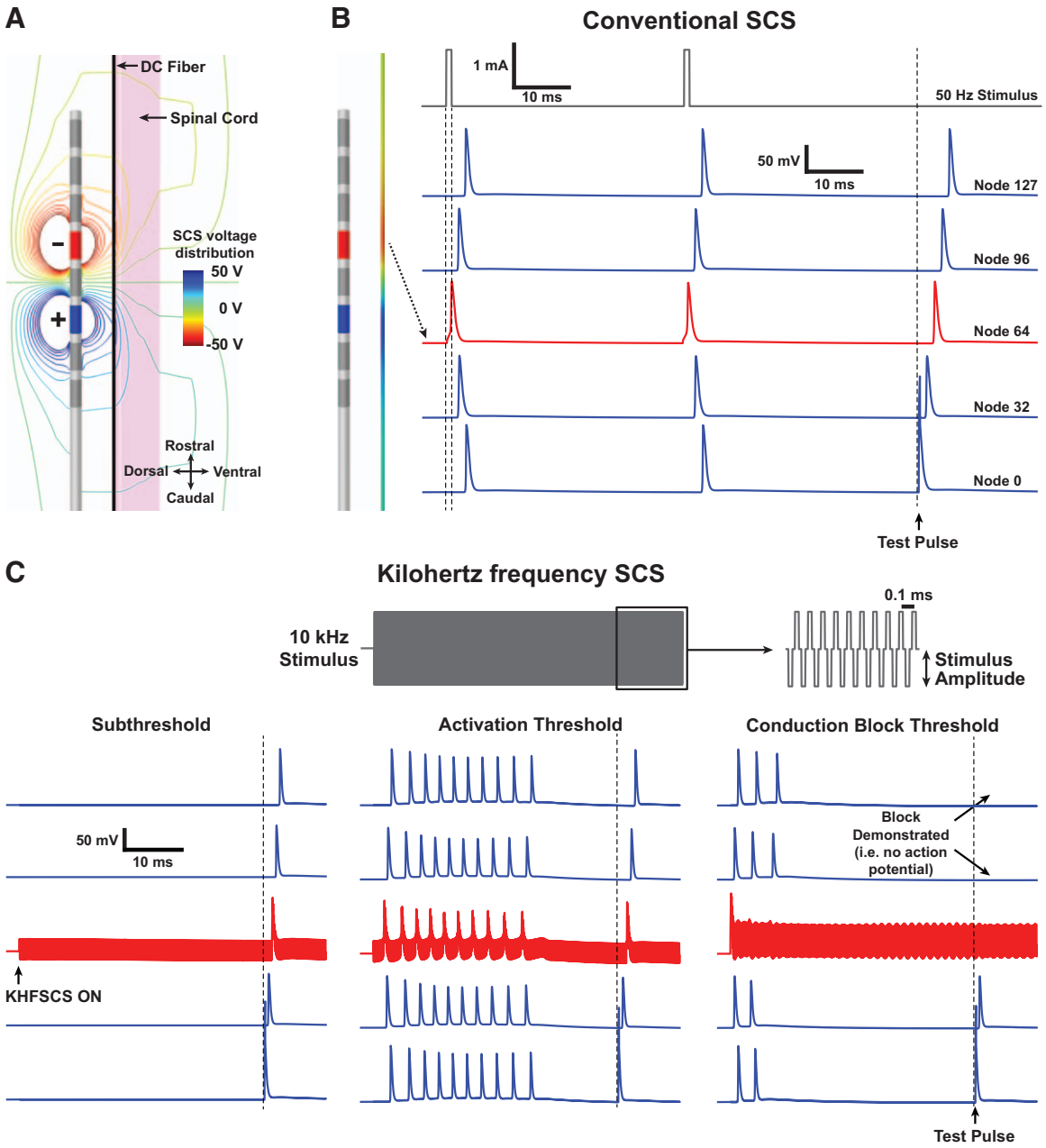

Fig. 2. Direct axonal response to kilohertz frequency spinal cord stimulation (KHFSCS). (*A*) Isopotential lines of the extracellular voltages generated by bipolar spinal cord stimulation (SCS). The voltage distributions were calculated from the finite element model. (*B*) To estimate the direct axonal response to SCS, the SCS-induced extracellular voltages were interpolated onto the axon models. With sufficient depolarization, action potentials were initiated in an axon and propagated in both directions. This figure shows the time-dependent transmembrane voltages at several nodes in a dorsal column (DC) axon model and illustrates action potential generation with a conventional 50-Hz SCS waveform. (*C*) The direct axonal response to KHFSCS was examined following the same procedure. Activation and conduction block thresholds were calculated for each axon model. The *left column* shows the time-dependent transmembrane voltages in an axon model in response to a subthreshold stimulus, whereas the *middle and right columns* demonstrate the responses to KHFSCS stimuli at activation and conduction block thresholds, respectively. To test for conduction block, a test pulse is applied at one end of the axon. This test pulse produces an action potential that propagates along the axon. If the KHFSCS amplitude is at or above the conduction block threshold, the action potential is unable to propagate past the stimulation electrode(s) (as demonstrated in the *right column*).

DR fibers (fig. 3). At the activation threshold, axons did not fire continuously but typically only generated a number of action potentials during the first 30 ms or less of KHFSCS (fig. 2C). However, it was possible to generate continuous firing at a rate of several hundred hertz with a range of stimulus amplitudes between the activation threshold and block

Table 2. List of Parameters for Each Group of Simulations

Waveform shape (fig. 3)	
Sinusoidal	**10 kHz; continuous**
Rectangular	**10 kHz; 30-μs pulse width; 20-μs interphase interval**
Target fibers	DC: 11.5-μm diameter DR: 15.0-μm diameter parent fiber; 11.5-μm diameter daughter fiber
Thresholds	Activation and block
Dorsal CSF thickness (fig. 4)	
Thickness	**2.0, 3.2, and 4.4 mm**
Target fibers	DC: 11.5 μm diameter DR: 15.0 μm diameter parent fiber; 11.5 μm diameter daughter fiber
KHFSCS waveform	Rectangular: 10 kHz; 30 μs pulse width; 20 μs interphase interval
Thresholds	Activation and block
Lead location (fig. 5)	
Distance between dura and lead (fig. 5A)	**0.0, 0.2, 0.4, 0.8, and 1.2 mm**
Lateral offset (fig. 5B)	**0.0, 1.0, 2.0, and 3.0 mm**
Target fibers	DC: 11.5 μm diameter DR: 15.0-μm diameter parent fiber; 11.5-μm diameter daughter fiber
KHFSCS waveform	Rectangular: 10 kHz; 30-μs pulse width; 20-μs interphase interval
Thresholds	Activation
Fiber collaterals (fig. 6A)	
Collateral diameter	**5.7, 7.3, and 11.5 μm**
Target fibers	DC: 11.5-μm diameter parent fiber
KHFSCS waveform	Rectangular: 10 kHz; 30-μs pulse width; 20-μs interphase interval
Thresholds	Activation
Fiber size (fig. 7)	
Axon diameter	**7.3, 11.5, and 15.0 μm**
Target fibers	DC
KHFSCS waveform	Rectangular: 10 kHz; 30-μs pulse width; 20-μs interphase interval
Thresholds	Activation and block

The free parameters are indicated in bold.

CSF = cerebrospinal fluid; DC = dorsal column; DR = dorsal root; KHFSCS = kilohertz frequency spinal cord stimulation.

threshold (data not shown). At the block threshold, KHFSCS also produced transient spiking, an effect referred to as the "onset response" (fig. 2C).[8]

Figure 3A shows contour plots of the activation and block thresholds for DC fibers as a function of position within the DC. Figure 3B shows the activation thresholds for DR fibers as function of rostrocaudal level of the DR and daughter DC fiber branch point relative to the center of the cathode. The sinusoidal waveform produced a minimum activation threshold and a block threshold of 4.7 and 8.4 mA, respectively, for DC fibers. For DR fibers, the sinusoidal waveform produced minimum activation and block thresholds of 4.6 and 9.2 mA, respectively. The rectangular waveform produced minimum activation and block thresholds of 4.6 and 8.0 mA, respectively, for DC fibers. For DR fibers, the rectangular waveform generated minimum activation and block thresholds of 4.3 and 8.5 mA, respectively. The conventional SCS waveform produced minimum excitation thresholds of 1.2 and 1.6 mA for DC and DR fibers, respectively.

Both of the KHFSCS waveforms had significantly higher activation thresholds relative to the conventional SCS waveform. However, the rectangular KHFSCS waveform required slightly lower amplitudes for activation and conduction block relative to the sinusoidal KHFSCS waveform. For a given amplitude, the rectangular KHFSCS waveform with a 30-μs pulse width also injected less charge per phase relative to the continuous sinusoidal KHFSCS waveform (*i.e.*, 6% difference). Therefore, we only present the rectangular KHFSCS waveform for the remaining analyses.

dCSF Thickness

The dorsal aspect of the spinal cord is separated from the dura by a layer of cerebrospinal fluid (fig. 4A). The thickness of this dCSF layer is believed to be one of the most important variables in determining therapeutic stimulation amplitudes in SCS as well as the ability to stimulate the desired neural targets.[35] The thickness of the dCSF varies significantly as a function of spinal level and is also highly variable between patients.[36] The middle and lower thoracic spinal levels have a thicker dCSF layer than other spinal levels, and higher amplitudes are required for therapeutic stimulation.[35] The thicker dCSF layer also makes it more difficult to activate the DC fibers without generating unwanted side effects due to activation of DR fibers.[37] Therefore, we examined the effects of dCSF thickness on activation and block thresholds in KHFSCS (fig. 4). Three thicknesses (2.0, 3.2, and 4.4 mm) were examined that largely covered the estimated range of the dCSF layer for the lower thoracic spinal cord (*i.e.*, 3.6 ± 1.6 mm at the T11 spinal level).[36]

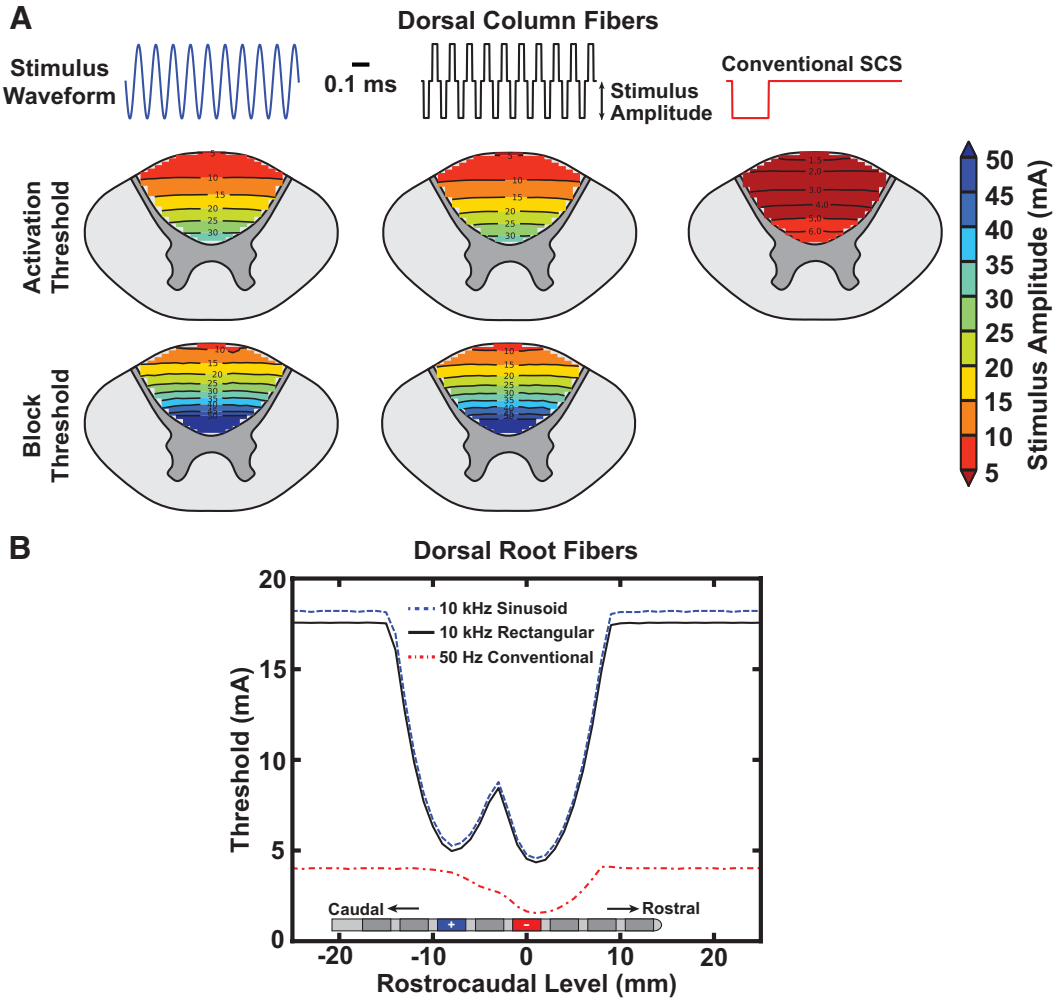

Fig. 3. Sinusoidal *versus* rectangular kilohertz frequency spinal cord stimulation (KHFSCS) waveforms. (*A*) Activation and conduction block thresholds for 11.5-μm diameter dorsal column (DC) fibers with sinusoidal and rectangular 10 kHz waveforms and activation thresholds with a conventional 50 Hz waveform. (*B*) Activation thresholds for dorsal root (DR) fibers with sinusoidal and rectangular 10 kHz waveforms and a conventional 50 Hz waveform as a function of rostrocaudal position of the DR branch point relative to the cathode. Both KHFSCS waveforms had significantly higher activation thresholds relative to the conventional spinal cord stimulation (SCS) waveform; however, the rectangular KHFSCS waveform resulted in slightly lower activation and block thresholds relative to the sinusoidal KHFSCS waveform. In this analysis, the 10-kHz rectangular waveform consisted of symmetric cathodic and anodic phases with pulse widths of 30 μs, separated by a 20-μs interpulse interval. The conventional 50 Hz waveform was monophasic with a pulse width of 210 μs.

Increases in dCSF thickness required higher KHFSCS amplitudes for activation and block in both DC and DR fibers in agreement with the clinical experience with conventional (approximately 50 Hz) SCS (fig. 4). For DC fibers, the minimum activation thresholds were 2.2, 4.6, and 8.2 mA and block thresholds were 3.9, 8.0, and 14.3 mA for dCSF thicknesses of 2.0, 3.2, and 4.4 mm (fig. 4C). For DR fibers, the minimum activation thresholds were 2.7, 4.3, and 6.4 mA and block thresholds were 5.5, 8.5, and 11.2 mA for dCSF thicknesses of 2.0, 3.2, and 4.4 mm (fig. 4C). For a thin dCSF layer (2.0 mm), there was a significant increase in the likelihood of DC and DR fiber activation, and it was possible to achieve conduction block of large-diameter DC fibers within the clinically relevant range (0.5 to 5 mA).[10]

Lead Location

This study considered KHFSCS with cylindrical leads that are typically implanted percutaneously with a Tuohy-style needle. When implanting these leads, much care is taken to place the leads at the desired rostrocaudal and mediolateral locations. However, it is difficult to control the dorsoventral position of the lead. In addition to the dorsoventral variability in lead location, it is also possible for the lead to be placed or migrate lateral to the spinal cord midline.

Because of the potential difficulties in controlling lead position, we examined the effects of electrode location on the activation thresholds for DC and DR fibers (fig. 5). To examine the effects of the dorsoventral position of the lead, we calculated the activation thresholds at a range of distances

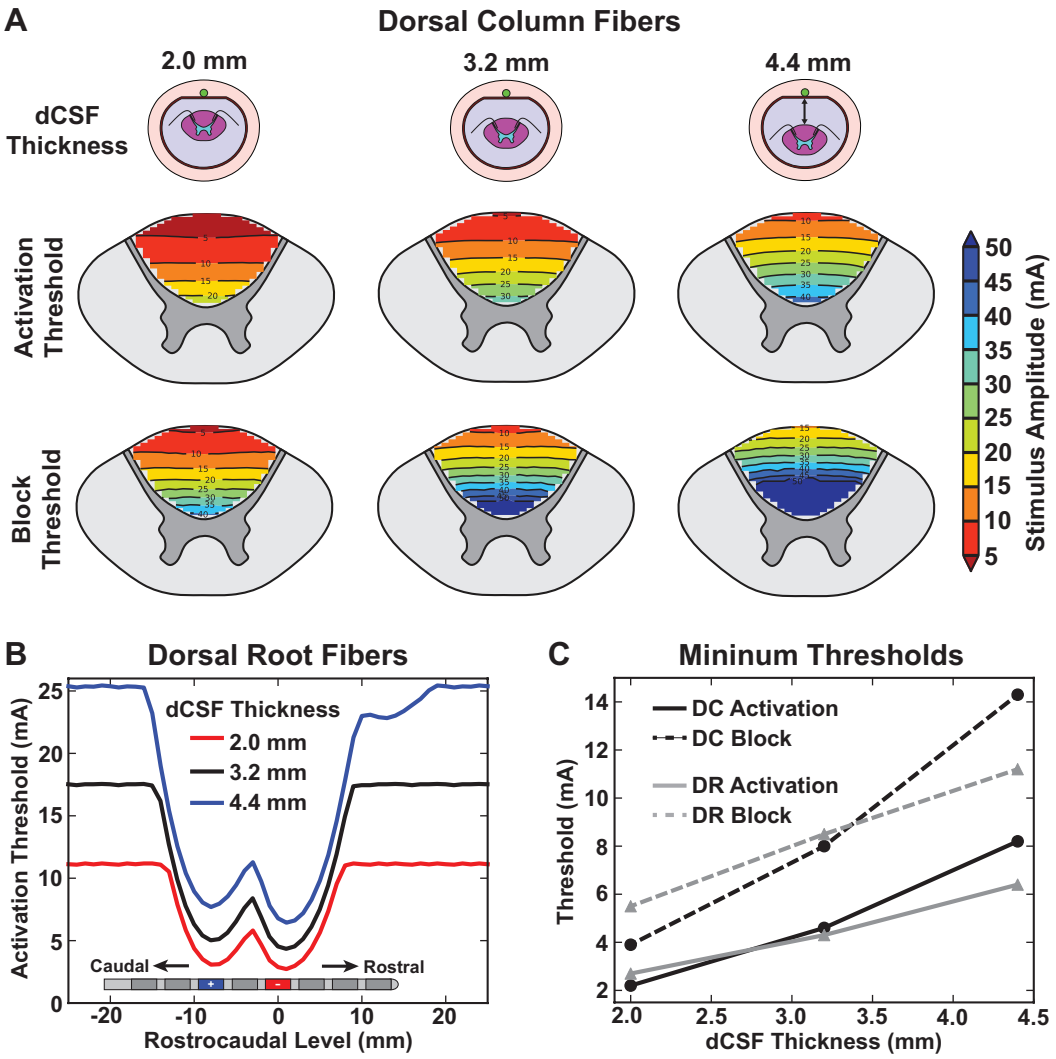

Fig. 4. Significance of dorsal cerebrospinal fluid (dCSF) layer thickness in kilohertz frequency spinal cord stimulation. (*A*) Dorsal column (DC) fiber activation and conduction block thresholds for dCSF layer thicknesses of 2.0, 3.2, and 4.4 mm are shown in the *left, middle, and right columns*, respectively. The *top row* shows the activation thresholds for each dCSF layer thickness, whereas the *bottom row* shows the corresponding conduction block thresholds. (*B*) Dorsal root (DR) fiber activation thresholds for each dCSF layer thickness as a function of rostrocaudal position of the DR branch point relative to the cathode. (*C*) Minimum thresholds for DC and DR fiber activation and conduction block as a function of dCSF layer thickness. In this analysis, DC fibers had a diameter of 11.5 μm.

between the dural surface and the lead surface (fig. 5A). For DC fibers, minimum activation thresholds were 4.6, 5.6, 6.3, 7.6, and 8.8 mA for distances of 0.0, 0.2, 0.4, 0.8, and 1.2 mm, respectively. For DR fibers, minimum activation thresholds were 4.3, 4.9, 5.3, 6.0, and 6.7 mA for distances of 0.0, 0.2, 0.4, 0.8, and 1.2 mm, respectively.

We also examined the effects of lateral lead migration by calculating the activation thresholds for a range of lateral lead offsets relative to the spinal cord midline (fig. 5B). For DC fibers, the minimum activation thresholds were 4.6, 4.7, 5.1, and 5.8 mA for distances of 0.0, 1.0, 2.0, and 3.0 mm. For DR fibers, the minimum activation thresholds were 4.3, 3.6, 3.3, and 3.3 mA at distances of 0.0, 1.0, 2.0, and 3.0 mm.

This analysis demonstrated that dorsoventral movement of the lead away from the dural surface resulted in an exponential increase in the activation thresholds for both DC and DR fibers. However, activation thresholds increased more rapidly for DC fibers relative to DR fibers. Lateral movement of the lead produced an exponential increase in the activation thresholds for DC fibers and an exponential decrease in the activation thresholds for DR fibers. Therefore, any movement of the stimulating lead away from the surface of the dura and/or the spinal cord midline increased the selective stimulation of DR fibers over DC fibers. These trends matched previous clinical and modeling results of conventional SCS.[37–39]

Fiber Collateralization

Dorsal column fibers are not simple straight axons, but they send out several collaterals at regularly spaced intervals that

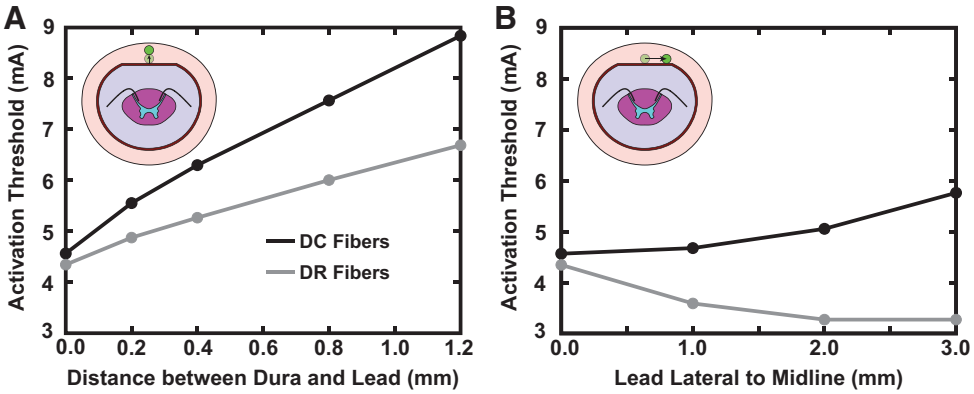

Fig. 5. Effects of lead position on kilohertz frequency spinal cord stimulation activation thresholds. (*A*) Minimum dorsal column (DC) and dorsal root (DR) fiber activation thresholds as a function of the distance between the dorsal surface of the dura and the spinal cord stimulation lead. Activation thresholds were calculated at distances of 0.0, 0.2, 0.4, 0.8, and 1.2 mm. (*B*) Minimum DC and DR fiber activation thresholds as a function of distance between the spinal cord midline and the center of the spinal cord stimulation lead. Activation thresholds were calculated at distances of 0.0, 1.0, 2.0, and 3.0 mm. In this analysis, DC fibers had a diameter of 11.5 μm.

project into the gray matter of the spinal cord where they freely arborize.[19,40] These projections occur at the nodes of Ranvier and can occur at an average spacing of approximately 1 mm, depending on the fiber type, fiber diameter, and distance from the corresponding DR fiber.[19,40] Modeling studies have shown that fiber collaterals lower conventional SCS activation thresholds by as much as 50%.[19] Therefore, we examined the effects of DC fiber collateralization on the activation thresholds during KHFSCS. We incorporated DC fiber collaterals that were oriented perpendicular to the rostrocaudal orientation of the parent DC fiber and projected in the ventral direction.

To examine the effects of DC fiber collateralization on activation thresholds during KHFSCS, the location of the lowest threshold DC fiber (*i.e.*, superficial DC fiber at the spinal cord midline) was varied along the rostrocaudal axis relative to the stimulating electrodes (fig. 6A). For an 11.5-μm diameter DC fiber, the collateral diameter was varied among 5.7, 7.3, and 11.5 μm (*i.e.*, fiber-to-collateral diameter ratios of 2.0, 1.6, and 1.0). The average fiber diameter-to-collateral diameter ratio has been estimated to be on the order of 3.1 ± 0.7 in Ia and Ib primary afferents originating from the cat hind limb muscles.[19,41] Smaller ratios (*i.e.*, larger collateral diameters) will produce a larger decrease in activation thresholds. Therefore, the range examined in this study represents an upper limit on activation threshold reduction due to DC fiber collateralization. Collateralization produced a maximum decrease in activation threshold of 0.0, 4.2, and 29.8% for fiber collateral diameters of 5.7, 7.3, and 11.5 μm, respectively (fig. 6A). Although Figure 6A shows that there was a significant reduction in the activation thresholds for a fiber-to-collateral diameter ratio of 1.0, the more physiologically relevant ratio of 2.0 (*i.e.*, collateral diameter of 5.7 μm) produced no decrease in activation threshold for a bipolar stimulation configuration.

The minimum thresholds occurred when the branching nodes were centered at the rostrocaudal level of the stimulating electrodes. There was an increase in activation threshold when the branching node was between the rostrocaudal level of the anode and cathode where the depolarizing force of the extracellular stimulation (*i.e.*, second spatial derivative of the extracellular voltages or activating function[42]) was close to zero (figs. 2A and 6A). Although clinical KHFSCS is performed with bipolar stimulation, we performed the same analysis for a monopolar stimulation configuration with a distant ground. Even under monopolar stimulation configurations, fiber collateralization produced a maximum threshold reduction from 5.7 to 5.3 mA (7.0%) for a fiber-to-collateral diameter ratio of 2.0 (data not shown).

The preceding analysis within the current section, "Fiber Collateralization," only considered a DC fiber with a single collateral; however, the presence of multiple collaterals can further decrease the activation thresholds.[19,43] Therefore, we also calculated the activation threshold during KHFSCS for a (11.5 μm diameter) DC parent fiber with 11 (5.7 μm diameter) collaterals at adjacent nodes of Ranvier. Multiple collaterals produced trends similar to those shown in figure 6A. For bipolar stimulation, there was no decrease in the activation thresholds, but a significant increase when the branching nodes were near the rostrocaudal levels of the stimulating electrodes (data not shown). For monopolar stimulation, the presence of these 11 collaterals produced a maximum threshold reduction from 5.7 to 5.2 mA (8.8%) (data not shown).

These small reductions in KHFSCS activation thresholds do not match previous conventional SCS modeling results that demonstrated a major reduction in DC activation threshold due to fiber collateralization for small-diameter fibers (6 μm) with smaller diameter collaterals (2 μm).[19] However, studies have shown that conventional SCS directly affects large-diameter fibers due to their low activation thresholds relative to small-diameter fibers.[21] Therefore, we investigated the effect of fiber collateralization for a range of fiber diameters (5.7 to 16.0 μm) with a fiber-to-collateral diameter ratio of 1.0 (*i.e.*, fiber diameter = collateral diameter). A single

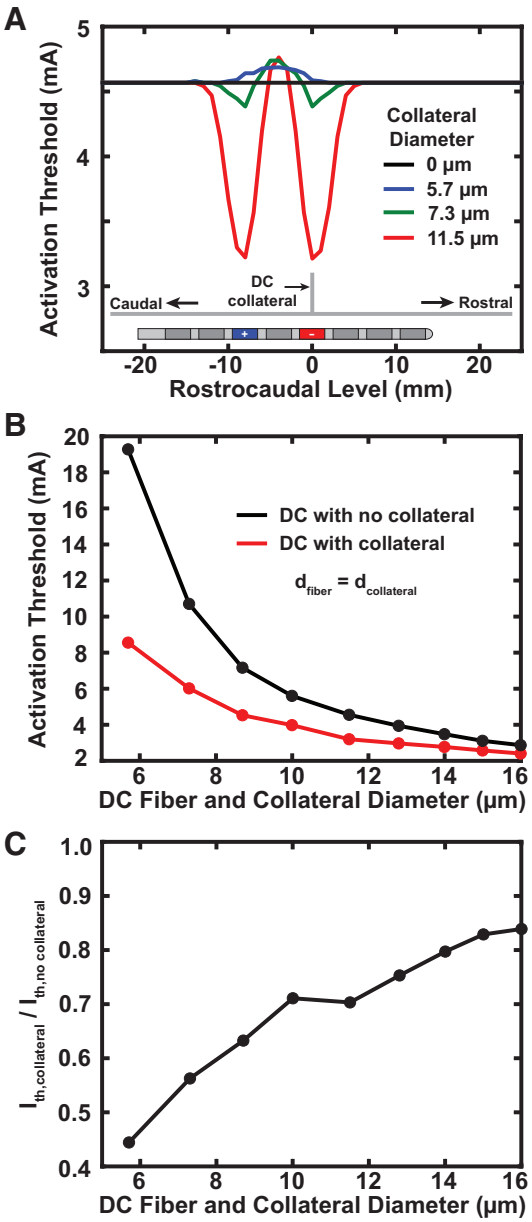

Fig. 6. Effects of dorsal column (DC) fiber collaterals on kilohertz frequency spinal cord stimulation activation thresholds. (*A*) DC fiber activation threshold as a function of collateral diameter. A single collateral was added to a 11.5-µm diameter DC fiber. The collateral diameter ($d_{collateral}$) was varied at 0.0, 5.7, 7.3, and 11.5 µm. For each $d_{collateral}$, the DC fiber activation threshold was calculated as a function of the rostrocaudal position of the branching node relative to the cathode. The DC collateral was oriented perpendicular to the parent DC fiber and projected ventrally away from the spinal cord stimulation lead. (*B* and *C*) Reduction in activation thresholds for DC fibers due to collateral branching as a function of fiber diameter. In this analysis, $d_{collateral}$ was assumed to equal the diameter of the parent DC fiber (d_{fiber}), and the branching node was centered at the rostrocaudal level of the cathode. (*B*) Shows the activation threshold for a range of fiber diameters with and without a collateral. (*C*) shows the relative ratio of activation threshold for a fiber with a collateral ($I_{th,collateral}$) to the activation threshold for the same fiber diameter with no collateral ($I_{th,no\ collateral}$).

fiber collateral produced a major reduction in activation threshold for small-diameter fibers, but this effect decreased with increasing fiber diameter (fig. 6, B and C).

Fiber Size

Extracellular electrical stimulation can excite myelinated axons by generating action potentials at the nodes of Ranvier. For myelinated fibers, the activation threshold is largely determined by the spacing between adjacent nodes of Ranvier.[44] This internodal spacing increases as a function of axon diameter, and therefore, large-diameter fibers have a lower threshold than smaller fibers. Previous studies suggest that conventional SCS functions through direct activation of large-diameter myelinated axons within the DC.[21] Therefore, fiber diameter is an important variable to consider in KHF-SCS because the DC of the human spinal cord consists of axons with a wide range of diameters (average fiber diameter approximately 5.0 µm and a maximum diameter of 16.0 µm at lower thoracic levels).[28] The density and distribution of fiber sizes are also a function of mediolateral position within the DC, with higher densities of medium-diameter and large-diameter fibers in the lateral DCs.[28] Therefore, activation and block thresholds were calculated for three DC fiber diameters (7.3, 11.5, and 15.0 µm) that represented a wide range of fiber diameters found within the human spinal cord and included large-diameter fibers that are most likely to be affected by SCS (fig. 7).[21,28] The results showed the expected trend of large-diameter fibers having the lowest activation and block thresholds. The minimum activation thresholds were 10.8, 4.6, and 3.1 mA for DC fiber diameters of 7.3, 11.5, and 15.0 µm, respectively (fig. 7B). The minimum block thresholds were 19.1, 8.0, and 5.5 mA for DC fiber diameters of 7.3, 11.5, and 15.0 µm, respectively (fig. 7B). The minimum DR fiber activation and block thresholds of 4.3 and 8.5 mA are also shown in figure 7B. This analysis shows that it is possible to have significant direct activation of large-diameter fibers (≥11.5 µm) within the current clinical range of stimulation amplitudes (0.5 to 5 mA).[10] However, even for the largest diameter fibers (15.0 µm), conduction block was not possible within the clinical range.

Discussion

Kilohertz frequency spinal cord stimulation for chronic pain management is a new and promising technology; however, recent clinical studies have presented conflicting results. Although it is possible that outcome inconsistency stems from clinical trial design and patient selection, it is also possible that clinical outcomes may have been affected by technical limitations, such as lead positioning and stimulation programming choices, and differences in the stimulation waveform parameters (*e.g.*, pulse width, frequency). Addressing such limitations can be challenging, particularly for KHFSCS, because it does not produce paresthesias.[9,11,12] Understanding the mechanisms responsible for the clinical benefits (or failure) of KHFSCS is critical to reduce variability

in how the therapy is delivered to the target neural elements. This knowledge will allow for future clinical studies to be more reproducible and to definitively answer efficacy questions. The present data represent a first step in this process and may be useful in KHFSCS therapy optimization.

KHFSCS Putative Mechanism: Direct Activation

This study used a computer model to characterize the effects of KHFSCS on spinal cord axons. Direct activation of spinal cord axons is one of the most obvious potential therapeutic mechanisms of KHFSCS. Therefore, we computed the KHFSCS thresholds for action potential generation under a number of conditions. In general, the results of this study suggest that KHFSCS requires significantly higher amplitudes for excitation relative to conventional approximately 50 Hz SCS (fig. 3). These amplitudes were often in the upper end or outside of the range currently used in clinical practice (*i.e.*, 0.5 to 5 mA).[10,12]

Regarding DC fibers, it was possible to excite large-diameter fibers (≥11.5 μm) within the clinical range, especially for a thin dCSF layer (*i.e.*, 2 mm) (fig. 4). However, any movement of the lead from the "ideal" location (*i.e.*, spinal cord midline and adjacent to the dural surface) resulted in an increase in the activation threshold (fig. 5). DC fiber collaterals have been shown to produce significant reductions in the stimulation amplitudes required for the activation of small-diameter fibers with conventional SCS.[19] In the current study, fiber collateralization of large-diameter DC fibers only produced a minor reduction in KHFSCS activation thresholds and increased activation thresholds at certain rostrocaudal levels for bipolar stimulation (fig. 6).

With respect to DR fibers, it was possible to excite large-diameter (15 μm) DR fibers within the clinical range of stimulus amplitudes, especially with a thin dCSF layer (2 mm) (fig. 4). As with DC fibers, dorsoventral movement of the lead away from the dural surface led to an increase in the DR fiber activation thresholds outside of the clinical range (fig. 5A). However, lateral displacement of the lead produced a moderate reduction in the DR fiber activation threshold (fig. 5B) and higher selectivity for stimulating DR fibers over DC fibers.

The data show that within the clinical range (0.5 to 5 mA), it is possible that KHFSCS leads to direct activation of

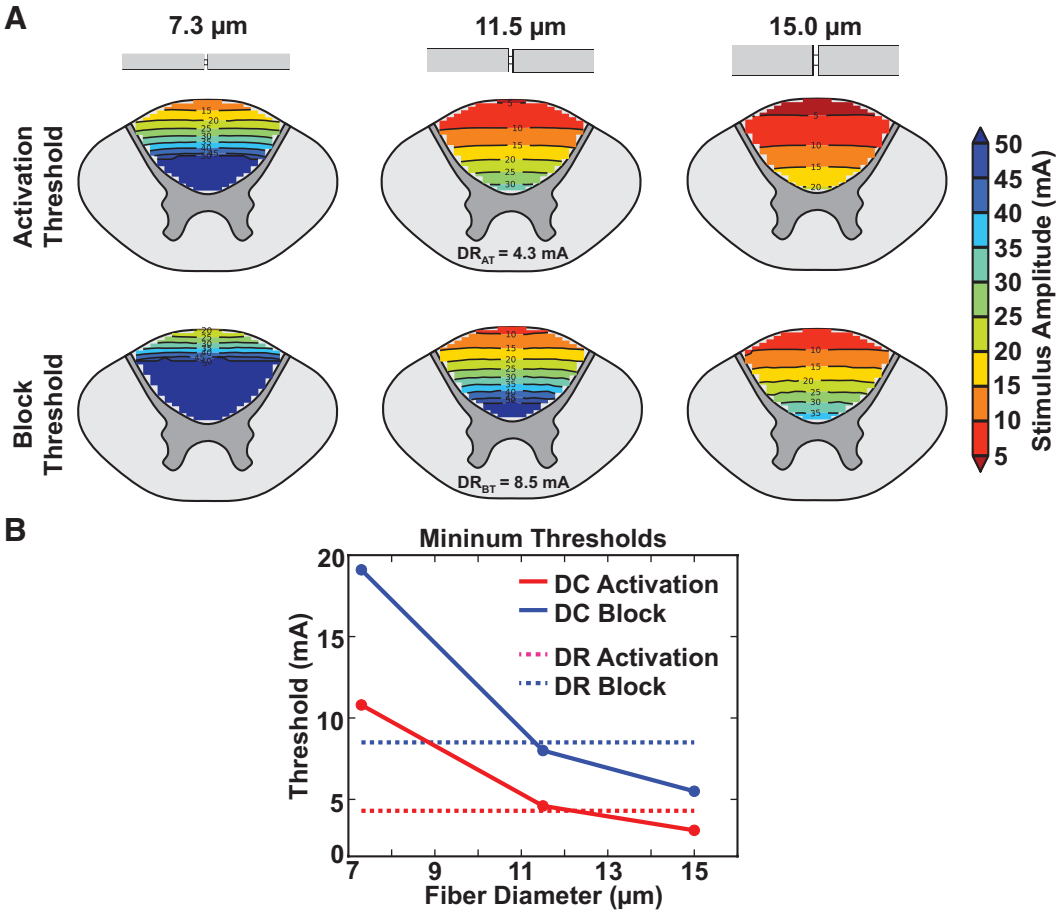

Fig. 7. Significance of fiber diameter in kilohertz frequency spinal cord stimulation. (*A*) Dorsal column (DC) fiber activation and conduction block thresholds for fiber diameters of 7.3, 11.5, and 15.0 μm are shown in the *left, middle, and right columns*, respectively. The *top row* shows the activation thresholds for each fiber size, whereas the *bottom row* shows the corresponding conduction block thresholds. (*B*) Minimum thresholds for DC fiber activation and conduction block for each fiber diameter. The minimum thresholds for dorsal root (DR) fiber activation (DR_{AT}) and conduction block (DR_{BT}) are also illustrated with the *dashed lines*.

large-diameter (≥11.5 μm) fibers in the superficial layer of the DC as well as large-diameter DR fibers close to the cathode or anode. Therefore, direct activation of spinal cord fibers may be a potential mechanism of action of KHFSCS. However, it is important to consider that the minimum activation thresholds (*i.e.*, most excitable fibers) were within the upper limits of this clinical range and above the clinically effective amplitudes reported in a small cohort of patients.[45] These coupled results reduce the likelihood that the clinical benefit thus far reported for KHFSCS[9–12] stems from direct activation of large-diameter spinal cord fibers. A lack of activation is also consistent with clinical evidence showing that, within the clinically effective amplitude range of 0.5 to 5 mA, patients do not experience the paresthesias that are a hallmark of DC or DR fiber activation.[10–12] Paresthesias are only generated at significantly higher amplitudes.[45] In turn, our theoretical predictions are in line with prior experimental evidence showing that KHFSCS does not modulate the firing rate of gracile nucleus neurons in a rat model of neuropathic pain.[15]

KHFSCS Putative Mechanism: Conduction Block

Direct conduction block of spinal cord fibers may be the most commonly assumed mechanism to mediate the effects of KHFSCS. This notion stems from prior studies that demonstrate conduction block generated by kilohertz frequency electrical stimulation in peripheral nerve models[6–8] as well as the lack of paresthesias reported in clinical studies.[9–12] We tested the thresholds for conduction block in DC and DR fibers under a number of different conditions. Conduction block thresholds were always higher than activation thresholds and this relation matched previous studies in the peripheral nervous system.[46] Conduction block thresholds were almost always outside of the clinical amplitude range, the only exception being large-diameter DC fibers when a very thin dCSF layer was assumed (2 mm) (fig. 3). However, the main current clinical application of KHFSCS involves stimulation at the lower thoracic (T8 to T11) levels which typically present a thicker dCSF layer.[35] The prediction that KHFSCS does not generate direct conduction block in the spinal cord matches prior observations. Before axonal conduction block is generated with kilohertz frequency stimulation, there is an initial increase in action potential firing in the target axons, called the "onset response."[8,46] This onset response can be observed experimentally during KHFSCS by recording increased activity in wide dynamic range neurons[34] and manifests behaviorally as several signs of discomfort for the first few minutes of stimulation that are different from the signs of sensory threshold.[14] Although this onset response has been observed in animal models of KHFSCS, no paresthesias or other subjective perceptions have been reported during clinically effective KHFSCS in human patients.[10]

Clinical and Mechanistic Implications

Although it is well accepted that conventional SCS functions through direct activation of spinal cord fibers,[47,48] the potential mechanisms of action of KHFSCS are unknown. The results of this study suggest that KHFSCS may not function explicitly through direct activation or conduction block of spinal cord fibers and may function through more complex or subtle mechanisms. There are a number of other potential mechanisms through which KHFSCS could provide pain relief. Some of these mechanisms include pseudospontaneous activation, transmission delays, or conduction failure at branch points. Pseudospontaneous activity is related to the concept that an individual neuron's response to a near-threshold stimulus may be subthreshold or suprathreshold due to the stochastic nature of ion channel gating.[49] Therefore, KHFSCS at subthreshold or near-threshold amplitudes may lead to asynchronous or pseudospontaneous activation of afferent fibers. KHFSCS may also alter the axonal response to incoming signals[14] or produce action potential conduction failure at axon branch points.[14,19,50–52] KHFSCS could potentially induce ion accumulation in the extracellular or periaxonal space that could affect activation and/or conduction block thresholds.[53,54] Last, paresthesia-free analgesia may not require KHFSCS, as it can also be achieved with conventional SCS waveforms applied in short bursts at 40 Hz.[55]

Study Limitations and Future Work

Although the KHFSCS model presented in this study was based on standard computational modeling principles, it was subject to a number of potential limitations, and its accuracy needs to be confirmed with future experimental and clinical studies. We only considered frequency-independent electrostatic solutions to the electric field generated during KHFSCS. It is possible that the frequency-dependent properties of the electrode–electrolyte interface of the stimulating electrodes as well as the surrounding biological tissue could affect the electric field generated during KHFSCS. We did not account for the potential effects of electrode encapsulation that could alter the electric field generated during KHFSCS.[22,56] However, the FEM did produce monopolar electrode impedances (430 Ω) that were within the clinically observed range for chronically implanted percutaneous SCS leads and activation thresholds with conventional 50 Hz SCS that were similar to a previously published computer model of SCS.[22]

We used a nonlinear axon model derived from mammalian motor axons[29] that may have a limited ability to represent the behavior of sensory neurons in the spinal cord. The axon model also was not explicitly parameterized for electrical stimulation rates in the kilohertz range. However, this axon model has shown a high degree of accuracy in reproducing the *in vivo* axonal response to kilohertz frequency electrical stimulation in the peripheral nervous system.[46]

Finally, this study represents a first step to describe the mechanisms that are more likely to mediate the clinical effects of KHFSCS. Future studies will be needed, and greater complexity will be added to include detailed axon branching,

synaptic terminals, cell bodies, and dendrites. Future work may examine the network effects of KHFSCS.[57,58] Future modeling studies could also be used to investigate optimized electrode designs, stimulation configurations, and waveform parameters that lower excitation/block thresholds and/or improve the ability to affect specific neural targets.

Conclusions

The results presented in this study represent significant strides toward theoretical characterization of the potential pain relief mechanisms of KHFSCS. Although a number of variables were considered, the activation and block thresholds for the most excitable fibers were in the upper limits or outside of the current clinical range of KHFSCS. Therefore, this study suggests that clinically effective KHFSCS may not function explicitly through direct activation or conduction block of spinal cord fibers and alternative concepts should be explored and evaluated.

Acknowledgments

The authors thank John T. Gale, Ph.D. (Neurosciences, Lerner Research Institute, Cleveland Clinic, Cleveland, Ohio), Hyun-Joo Park, Ph.D. (Center for Neurological Restoration, Cleveland Clinic), and Aaron J. Fleischman, Ph.D. (Biomedical Engineering, Lerner Research Institute, Cleveland Clinic), for their assistance with the finite element modeling. The authors also thank Niloy Bhadra, M.D., Ph.D. (Biomedical Engineering, Case Western Reserve University, Cleveland, Ohio), and Narendra Bhadra, Ph.D. (Neural Engineering Center, Case Western Reserve University), for their helpful discussions with kilohertz frequency electrical stimulation of neural tissue, and Kabilar Gunalan, M.S. (Biomedical Engineering, Case Western Reserve University), for his assistance running the NEURON simulations. The authors also thank Michael A. Moffitt, Ph.D. (Neuromodulation Research and Advanced Concepts, Boston Scientific Neuromodulation, Valencia, California), for his helpful comments and discussion.

This work was supported by the Louis Stokes Cleveland Veterans Affairs Medical Center, Cleveland, Ohio.

Competing Interests

Dr. Kilgore has equity ownership in Neuros Medical, Inc. (Willoughby Hills, Ohio). Dr. McIntyre is a paid consultant for Boston Scientific Neuromodulation (Valencia, California) and is a shareholder in the following companies: Surgical Information Sciences, Inc. (Minneapolis, Minnesota); Autonomic Technologies, Inc. (Redwood City, California); Cardionomics, Inc. (Forest Lake, Minnesota); Neuros Medical, Inc.; and Enspire DBS Therapy, Inc. (Wilmington, Delaware). Dr. Machado has the following disclosures: distribution rights from intellectual property for Enspire DBS Therapy, Inc., Autonomic Technologies, Inc., and Cardionomics, Inc.; consultant for Icahn School of Medicine at Mount Sinai (New York, New York), Spinal Modulation (Menlo Park, California), and Functional Neuromodulation (St. Paul, Minnesota); and fellowship program support from Medtronic, Inc. (Minneapolis, Minnesota). Dr. Lempka declares no competing interests.

Correspondence

Address correspondence to Dr. Lempka: Center for Neurological Restoration, Cleveland Clinic, 9500 Euclid Avenue (S31), Cleveland, Ohio 44195. lempkas@ccf.org.

Appendix. Model Details

Finite Element Analysis of KHFSCS

Additional Geometrical Parameters of the FEM. Unless specified otherwise, the dorsal cerebrospinal fluid layer had a thickness of 3.2 mm, a value within the range clinically observed at the lower thoracic levels.[36] The dura thickness was set to 300 μm, and its dorsal surface was flattened for computational simplicity.[22,59] Each electrode contact had a diameter of 1.25 mm and length of 3 mm and were separated from adjacent electrodes by electrode insulation 1 mm in length.

FEM Design and Electric Field Calculations. The model geometry was defined and meshed with the 3-matic Module within the Mimics Innovation Suite (Materialise, Belgium). We specified higher mesh densities near the electrode array as well as within a 35-mm long region of interest surrounding the electrode array. The total model length was 201 mm with a diameter of 70 mm. The FEM consisted of more than 12.7 million first-order tetrahedral elements. After the model geometry and mesh were generated, it was exported to the FEM software package, COMSOL Multiphysics (COMSOL, Inc., U.S.A.). Within COMSOL, electrical conductivities were assigned to each domain based on experimental data available in the literature (Table 1).[21,22,26]

In this study, all simulations were performed for bipolar stimulation applied through two active contacts separated by an inactive contact (i.e., separation of 8 mm center-to-center) (fig. 1A). We selected a distance of 8 mm between the anode and cathode because it represents common clinical programming selections in spinal cord stimulation. To calculate the electric fields generated by bipolar KHFSCS, we placed unit current sources (i.e., 1 A) of opposite polarity at the cathode and anode and set the outer surfaces of the general thorax layer to ground (i.e., 0 V) (fig 1A). We then calculated the voltage distributions (Φ) generated in the tissue (stiffness matrix, σ) based on the specified current sources (I) by solving the Poisson equation:

$$\nabla \cdot \sigma \nabla \Phi = -I$$

We calculated electrostatic FEM solutions for these unit current sources with an iterative equation solver using the conjugate gradient method. We refined the mesh density until further increasing the mesh density produced a maximum of less than 2% difference in the activation thresholds calculated for the neural elements considered in this study. Doubling the total volume of the FEM produced a maximum of less than 2% difference in the predicted activation thresholds.

Axon Models

We represented dorsal column (DC) and dorsal root (DR) fibers with a previously published compartmental model of a mammalian motor axon.[29] This model reproduces experimental data by

accurately representing the ion channels at the nodes of Ranvier as well as matching the geometry of the paranode, internode, and myelin to measured morphology. This model incorporates a double-layer cable model that accounts for the finite impedance of the myelin sheath. The nodes of Ranvier contain fast Na^+, persistent Na^+, and slow K^+ nonlinear conductances as well as the linear leakage conductance and the membrane capacitance. All equations and parameters for the axon model were defined in the study by McIntyre *et al.*[29] Unless specified otherwise, each DC fiber was 159 mm long with a fiber diameter of 11.5 μm and 128 nodes of Ranvier. For the DR fibers, the mother fiber had a diameter of 15.0 μm and a length of 43.5 mm with 31 nodes of Ranvier. The daughter DC fiber had a diameter of 11.5 μm and a length of 118 mm with 95 nodes of Ranvier.

The lengths of the DC and DR fibers were sufficient to ignore potential edge effects that can occur due to the wide mean membrane depolarization that occurs during kilohertz frequency stimulation.[46] Simulations were performed with the software package, NEURON, within the Python programming environment.[60] Model solutions were calculated using backward Euler implicit integration with a time step of 0.002 ms.

Simulation Procedures

To assess the direct neural response to KHFSCS, the voltage distributions calculated in the FEM were ported to the Python programming environment and directly applied to the axon models of the DC and DR fibers. Because the bulk conductivity (σ) is linear, the voltage distributions generated by different current source waveforms or magnitudes were scaled versions of the original FEM solutions with unit currents. The scaled voltage distributions were interpolated onto the model neurons described above using the extracellular mechanism within NEURON. The activation and block thresholds were determined using a bisection algorithm (error < 0.1 mA).

References

1. Shealy CN, Mortimer JT, Reswick JB: Electrical inhibition of pain by stimulation of the dorsal columns: Preliminary clinical report. Anesth Analg 1967; 46:489–91
2. Kumar K, Bishop S: Financial impact of spinal cord stimulation on the healthcare budget: A comparative analysis of costs in Canada and the United States. J Neurosurg Spine 2009; 10:564–73
3. North RB, Kidd DH, Piantadosi S: Spinal cord stimulation *versus* reoperation for failed back surgery syndrome: A prospective, randomized study design. Acta Neurochir Suppl 1995; 64:106–8
4. Kemler MA, Barendse GA, van Kleef M, de Vet HC, Rijks CP, Furnée CA, van den Wildenberg FA: Spinal cord stimulation in patients with chronic reflex sympathetic dystrophy. N Engl J Med 2000; 343:618–24
5. Kumar K, Taylor RS, Jacques L, Eldabe S, Meglio M, Molet J, Thomson S, O'Callaghan J, Eisenberg E, Milbouw G, Buchser E, Fortini G, Richardson J, North RB: The effects of spinal cord stimulation in neuropathic pain: A 24-month follow-up of the prospective randomized controlled multicenter trial of the effectiveness of spinal cord stimulation. Neurosurgery 2008; 63:762–70
6. Joseph L, Butera RJ: High-frequency stimulation selectively blocks different types of fibers in frog sciatic nerve. IEEE Trans Neural Syst Rehabil Eng 2011; 19:550–7
7. Tai C, Guo D, Wang J, Roppolo JR, de Groat WC: Mechanism of conduction block in amphibian myelinated axon induced by biphasic electrical current at ultra-high frequency. J Comput Neurosci 2011; 31:615–23
8. Kilgore KL, Bhadra N: Reversible nerve conduction block using kilohertz frequency alternating current. Neuromodulation 2014; 17:242–54; discussion 254–5
9. Van Buyten JP, Al-Kaisy A, Smet I, Palmisani S, Smith T: High-frequency spinal cord stimulation for the treatment of chronic back pain patients: Results of a prospective multicenter European clinical study. Neuromodulation 2013; 16:59–65; discussion 65–6
10. Tiede J, Brown L, Gekht G, Vallejo R, Yearwood T, Morgan D: Novel spinal cord stimulation parameters in patients with predominant back pain. Neuromodulation 2013; 16:370–5
11. Al-Kaisy A, Van Buyten JP, Smet I, Palmisani S, Pang D, Smith T: Sustained effectiveness of 10 kHz high-frequency spinal cord stimulation for patients with chronic, low back pain: 24-month results of a prospective multicenter study. Pain Med 2014; 15:347–54
12. Russo M, Van Buyten JP: 10-kHz high-frequency SCS therapy: A clinical summary. Pain Med 2014; [Epub ahead of print]
13. Perruchoud C, Eldabe S, Batterham AM, Madzinga G, Brookes M, Durrer A, Rosato M, Bovet N, West S, Bovy M, Rutschmann B, Gulve A, Garner F, Buchser E: Analgesic efficacy of high-frequency spinal cord stimulation: A randomized double-blind placebo-controlled study. Neuromodulation 2013; 16:363–9; discussion 369
14. Shechter R, Yang F, Xu Q, Cheong YK, He SQ, Sdrulla A, Carteret AF, Wacnik PW, Dong X, Meyer RA, Raja SN, Guan Y: Conventional and kilohertz-frequency spinal cord stimulation produces intensity- and frequency-dependent inhibition of mechanical hypersensitivity in a rat model of neuropathic pain. Anesthesiology 2013; 119:422–32
15. Song Z, Viisanen H, Meyerson BA, Pertovaara A, Linderoth B: Efficacy of kilohertz-frequency and conventional spinal cord stimulation in rat models of different pain conditions. Neuromodulation 2014; 17:226–34; discussion 234–5
16. Sin WK, Coburn B: Electrical stimulation of the spinal cord: A further analysis relating to anatomical factors and tissue properties. Med Biol Eng Comput 1983; 21:264–9
17. Coburn B, Sin WK: A theoretical study of epidural electrical stimulation of the spinal cord—Part I: Finite element analysis of stimulus fields. IEEE Trans Biomed Eng 1985; 32:971–7
18. Coburn B: A theoretical study of epidural electrical stimulation of the spinal cord-Part II: Effects on long myelinated fibers. IEEE Trans Biomed Eng 1985; 32:978–86
19. Struijk JJ, Holsheimer J, van der Heide GG, Boom HB: Recruitment of dorsal column fibers in spinal cord stimulation: Influence of collateral branching. IEEE Trans Biomed Eng 1992; 39:903–12
20. Struijk JJ, Holsheimer J, Boom HB: Excitation of dorsal root fibers in spinal cord stimulation: A theoretical study. IEEE Trans Biomed Eng 1993; 40:632–9
21. Holsheimer J: Which neuronal elements are activated directly by spinal cord stimulation. Neuromodulation 2002; 5:25–31
22. Lee D, Hershey B, Bradley K, Yearwood T: Predicted effects of pulse width programming in spinal cord stimulation: A mathematical modeling study. Med Biol Eng Comput 2011; 49:765–74
23. Capogrosso M, Wenger N, Raspopovic S, Musienko P, Beauparlant J, Bassi Luciani L, Courtine G, Micera S: A computational model for epidural electrical stimulation of spinal sensorimotor circuits. J Neurosci 2013; 33:19326–40
24. Chandrupatla TR, Belegundu AD: Introduction to Finite Elements in Engineering, 4th edition. Upper Saddle River, Pearson, 2012
25. Kameyama T, Hashizume Y, Sobue G: Morphologic features of the normal human cadaveric spinal cord. Spine (Phila Pa 1976) 1996; 21:1285–90

26. Ladenbauer J, Minassian K, Hofstoetter US, Dimitrijevic MR, Rattay F: Stimulation of the human lumbar spinal cord with implanted and surface electrodes: A computer simulation study. IEEE Trans Neural Syst Rehabil Eng 2010; 18:637–45
27. Ranck JB Jr: Which elements are excited in electrical stimulation of mammalian central nervous system: A review. Brain Res 1975; 98:417–40
28. Feirabend HK, Choufoer H, Ploeger S, Holsheimer J, van Gool JD: Morphometry of human superficial dorsal and dorsolateral column fibres: Significance to spinal cord stimulation. Brain 2002; 125(Pt 5):1137–49
29. McIntyre CC, Richardson AG, Grill WM: Modeling the excitability of mammalian nerve fibers: Influence of afterpotentials on the recovery cycle. J Neurophysiol 2002; 87:995–1006
30. Carpenter MB: Core Text of Neuroanatomy. Baltimore, Williams & Wilkins, 1991
31. Holsheimer J, Buitenweg JR, Das J, de Sutter P, Manola L, Nuttin B: The effect of pulsewidth and contact configuration on paresthesia coverage in spinal cord stimulation. Neurosurgery 2011; 68:1452–61
32. North RB, Kidd DH, Zahurak M, James CS, Long DM: Spinal cord stimulation for chronic, intractable pain: Experience over two decades. Neurosurgery 1993; 32:384–94; discussion 394–5
33. Yearwood TL, Hershey B, Bradley K, Lee D: Pulse width programming in spinal cord stimulation: A clinical study. Pain Physician 2010; 13:321–35
34. Cuellar JM, Alataris K, Walker A, Yeomans DC, Antognini JF: Effect of high-frequency alternating current on spinal afferent nociceptive transmission. Neuromodulation 2013; 16:318–27; discussion 327
35. He J, Barolat G, Holsheimer J, Struijk JJ: Perception threshold and electrode position for spinal cord stimulation. Pain 1994; 59:55–63
36. Holsheimer J, den Boer JA, Struijk JJ, Rozeboom AR: MR assessment of the normal position of the spinal cord in the spinal canal. AJNR Am J Neuroradiol 1994; 15:951–9
37. Manola L, Holsheimer J: Technical performance of percutaneous and laminectomy leads analyzed by modeling. Neuromodulation 2004; 7:231–41
38. Struijk JJ, Holsheimer J, Barolat G, He J, Boom HBK: Paresthesia thresholds in spinal cord stimulation—A comparison of theoretical results with clinical data. IEEE Trans Rehabil Eng 1993; 1:101–8
39. Alò K, Varga C, Krames E, Prager J, Holsheimer J, Manola L, Bradley K: Factors affecting impedance of percutaneous leads in spinal cord stimulation. Neuromodulation 2006; 9:128–35
40. Fyffe REW: Afferent fibers, Handbook of the Spinal Cord, Vols. 2 & 3—Anatomy and Physiology. Edited by Davidoff RA. New York, Dekker, 1984, pp 79–136
41. Hongo T, Kudo N, Sasaki S, Yamashita M, Yoshida K, Ishizuka N, Mannen H: Trajectory of group Ia and Ib fibers from the hind-limb muscles at the L3 and L4 segments of the spinal cord of the cat. J Comp Neurol 1987; 262:159–94
42. Moffitt MA, Lee DC, Bradley K: Spinal Cord Stimulation: Engineering Approaches to Clinical and Physiological Challenges, Implantable Neural Prostheses 1. New York, Springer US, 2009, pp 155–94
43. Danner SM, Hofstoetter US, Ladenbauer J, Rattay F, Minassian K: Can the human lumbar posterior columns be stimulated by transcutaneous spinal cord stimulation? A modeling study. Artif Organs 2011; 35:257–62
44. Rattay F: Analysis of models for external stimulation of axons. IEEE Trans Biomed Eng 1986; 33:974–7
45. Al-Kaisy A, Palmisani S, Smith T, Harris S, Pang D: The use of 10-kilohertz spinal cord stimulation in a cohort of patients with chronic neuropathic limb pain refractory to medical management. Neuromodulation 2015; 18:18–23
46. Bhadra N, Lahowetz EA, Foldes ST, Kilgore KL: Simulation of high-frequency sinusoidal electrical block of mammalian myelinated axons. J Comput Neurosci 2007; 22:313–26
47. Guan Y: Spinal cord stimulation: Neurophysiological and neurochemical mechanisms of action. Curr Pain Headache Rep 2012; 16:217–25
48. Smits H, van Kleef M, Holsheimer J, Joosten EA: Experimental spinal cord stimulation and neuropathic pain: Mechanism of action, technical aspects, and effectiveness. Pain Pract 2013; 13:154–68
49. Rubinstein JT, Wilson BS, Finley CC, Abbas PJ: Pseudospontaneous activity: Stochastic independence of auditory nerve fibers with electrical stimulation. Hear Res 1999; 127:108–18
50. Zhou L, Chiu SY: Computer model for action potential propagation through branch point in myelinated nerves. J Neurophysiol 2001; 85:197–210
51. Grill WM, Cantrell MB, Robertson MS: Antidromic propagation of action potentials in branched axons: Implications for the mechanisms of action of deep brain stimulation. J Comput Neurosci 2008; 24:81–93
52. Debanne D, Campanac E, Bialowas A, Carlier E, Alcaraz G: Axon physiology. Physiol Rev 2011; 91:555–602
53. Bellinger SC, Miyazawa G, Steinmetz PN: Submyelin potassium accumulation may functionally block subsets of local axons during deep brain stimulation: A modeling study. J Neural Eng 2008; 5:263–74
54. Ackermann DM, Bhadra N, Gerges M, Thomas PJ: Dynamics and sensitivity analysis of high-frequency conduction block. J Neural Eng 2011; 8:065007
55. De Ridder D, Plazier M, Kamerling N, Menovsky T, Vanneste S: Burst spinal cord stimulation for limb and back pain. World Neurosurg 2013; 80:642–649.e1
56. Arle JE, Carlson KW, Mei L, Shils JL: Modeling effects of scar on patterns of dorsal column stimulation. Neuromodulation 2014; 17:320–33; discussion 333
57. Arle JE, Carlson KW, Mei L, Iftimia N, Shils JL: Mechanism of dorsal column stimulation to treat neuropathic but not nociceptive pain: Analysis with a computational model. Neuromodulation 2014; 17:642–55; discussion 655
58. Zhang TC, Janik JJ, Grill WM: Modeling effects of spinal cord stimulation on wide-dynamic range dorsal horn neurons: Influence of stimulation frequency and GABAergic inhibition. J Neurophysiol 2014; 112:552–67
59. Manola L, Roelofsen BH, Holsheimer J, Marani E, Geelen J: Modelling motor cortex stimulation for chronic pain control: Electrical potential field, activating functions and responses of simple nerve fibre models. Med Biol Eng Comput 2005; 43:335–43
60. Hines ML, Davison AP, Muller E: NEURON and Python. Front Neuroinform 2009; 3:1